

NATURAL ANTIBIOFOULING AGENTS AS NEW CONTROL METHOD FOR PHOTOTROPHIC BIOFILMS DWELLING ON MONUMENTAL STONE SURFACES

Oana-Adriana CUZMAN*, Mara CAMAITI, Barbara SACCHI, Piero TIANO

CNR-ICVBC Istituto per la Conservazione e la Valorizzazione dei Beni Culturali, Sesto Fiorentino, Italy

Abstract

Five natural antibiofoulants with terrestrial (capsaicine - CS, cinnamaldehyde - CI) and marine origin (zosteric acid - ZA, poly-alkylpyridinium salts - pAPS and Ceramium botryocarpum extract - CBE) have been selected and tested against phototrophic biofilm formation on the stone surfaces for their inhibitory properties. The antibiofouling agents (ABAs) were incorporated into two commercial silicone based coatings (Silres BS OH 100 - S and Silres BS 290 - W). In this work, phototrophic growth was evaluated by epifluorescence microscopy and semi-quantitative image analysis. The results showed an inhibitory efficiency for almost all tested ABAs. However, this efficiency has been found for short time or when the incorporating agent were incompletely cured. Among the ABAs tested, the poly-alkylpyridinium salts and cinnamaldehyde incorporated into Silres BS 290 showed the best inhibitory efficiency.

Keywords: antifouling; biofouling; biodeterioration; phototrophic biofilm; natural antifoulants.

Introduction

The biological colonization can occur on almost all types of materials and also the man-made structures and artifacts are exposed to biodeteriogenic processes. This problematic is particular evident in the field of Monumental Heritage. In fact, it is well known that the microbial colonization of stones commonly starts with phototrophic organisms which build up a visible biofilm enriched with inorganic and organic biomass [1]. Once established, the phototrophic biocenosis allow the growth of more complex microbial consortia formed by heterotrophic microorganisms and therefore participate directly in decay processes, causing firstly aesthetic and subsequently structural damages [2].

The fouling is a widespread phenomenon and some organisms may be heavily fouled, while others can be totally fouling-free. This has generated high interest in identifying the biological metabolites that might repel or inhibit fouling organisms. These natural antifouling agents are active substances found in marine animals, plants microorganisms, and in terrestrial plants, which prevent the settlement of microorganisms and the patina formation on the surface of their structures, and they are believed to function as natural chemical defence against fouling [3, 4]. These natural substances are based on toxic or inhibitory compounds, having an antimicrobial, repellent or repressive action against biological settlement. These biomolecules are considered a potential environmental friendly agent for developing novel active ingredients

* Corresponding author: cuzman@icvbc.cnr.it

in antifouling coating preparations [5, 6]. Recent studies in the marine biofouling sector consider the fluoropolymers and silicones the best materials that can be used as fouling-release coatings [7]. For example, silicones coatings with encapsulated zosteric acid or capsaicin were currently investigated to achieve their slow release for prevent freshwater bacterial attachment [8-12].

This paper aimed to evaluate the efficacy of five natural products against the phototrophic biofilm formation on monumental heritage, in order to postpone the microbial colonization on the stone surfaces which are exposed to favorable biological growth conditions. A set of antibiofouling agents (ABAs) were selected among those described in literature, which showed ability to inhibit the biofilm formation, and tested by mixing them with two commercial silicon based polymers, Silres BS OH 100 - S and Silres BS 290 – W. Three of them are present in marine environment: poly-alkylpyridinium salts (pAPS) isolated from the marine sponge *Reniera sarai* [13, 14], zosteric acid (ZA) present in the eel grass *Zostera marina* [12,15] and a dichloromethane extract of *Ceramium botryocarpum* (CBE) marine rhodophyta [16]. The other two antifoulants selected for this study have a terrestrial origin: capsaicin (CS), the natural extract from chilli pepper [11, 17], and cinnamaldehyde (CI) present in cinnamon bark [18, 19]. The epifluorescence microscopy [20] and image-analysing software ImageJ® [21] were chosen for evaluating their efficiency by measuring the area covered by the phototrophic patina on stone specimens, while the ESEM-EDX method was used for observe the surface morphology of the coatings. The selected ABAs were characterised by FT-IR spectroscopy.

Materials and methods

Stone material

The experiments were carried out using Sivec marble, a white metamorphic dolomitic stone with porosity of 0.50 %, and medium grain size with unimodal pore size distribution. The dimension of the specimens used was of 5x5x1cm (indoor exposition) and 1x1x0.5cm and 5x5x1cm (outdoor exposition).

Antifouling agents and coating preparation

Most of the ABAs show high water solubility, and some of them are also soluble in organic solvents (i.e. methyl or ethyl alcohol). The mixing of the ABAs with the commercial coatings, which are reactive and/or immiscible with water, has required preliminary mixing tests in order to evaluate the best operative conditions. In all case the mixture ABAs/coating was used within one hour from the preparation. The ABAs concentration and the solvent used for the preparation of the ABAs mixtures are reported in Table 1. The five natural antibiofouling agents (ABAs), the biocide used as reference (A) and the incorporating agents (S and W) that have been selected and tested as potential inhibitors of phototrophic biofilm formation are reported below:

- Poly-alkyl-pyridinium salts (pAPS) (*3-alkylpyridinium* active compound) is chemically similar to alkyl ammonium compounds. It was used only in water solution.
- Zosteric acid (ZA) (*p-sulphoxy-cinnamic acid*) was synthesised according to the procedure reported in literature [22]. The purification of the product was performed only by extraction in diethyl ether and dissolution in methanol. The ESI-MS and FT-IR analyses of the final product were in agreement with the presence of zosteric acid. It was used in water or methanol solution.
- The active compound of the *Ceramium botryocarpum* extract (CBE) is still unknown. Very recent studies report the presence of salt of natural digeneaside in the red alga *Ceramium botryocarpum* extracts [23]. It was used in water or methanol solution.

- Capsaicin (CS) (*8-methyl-N-vanillyl-6-nonenamide*) employed in this study was purchased from Aldrich Chemical Co., and its composition was 65% capsaicin and 35% dihydrocapsaicin. It was used in water or ethanol solution [24].
- Cinnamaldehyde (CI) (*trans-3-phenyl-2-propenal*) was purchased from Aldrich Chemical Co., and it was used only in methanol solution.
- Concentrate Algophase (A) (*N-butyl-1,2 benzisothiazolin-3-one*) is a commercial biocide with a large spectrum of action (brown and green algae, lichens, fungi, bacteria) that was used as positive control although this product has a biocide action and not an antibiofouling one [25]. It was used as supplied.
- Silres BS OH 100 (S) is ethyl-silicate, solventless product and ready-to-use as light consolidant for construction materials. It was purchased from Waker Chemie A.G..
- Silres BS 290 (pure W) is solventless concentrate alkyl alkoxysilanes oligomer, based on a silane/siloxane mixture and commonly used as water-repellent for stone substrates. The product was diluted in 2-Propanol (W) (7%, v/v). It was purchased from Waker Chemie A.G.

Table 1. Operative condition of the experiments

ABAs	ABAs concentration (g/100 ml) in solvent	Coating	Curing period (days)	ABAs concentration in coatings	Samples exposition	ABAs solution/coating solution (ml/ml)
pAPS	0.0114 water	W	5	0.001 % w/v	indoor	1.75/18.25
			5; 30	0.003 % w/v	outdoor	5.26/14.74
CBE	2 methanol	S	5	0.06 % w/v	indoor	0.6/19.4
			5	0.2 % w/v	outdoor	2/18
ZA	2 water	W	5	0.06 % w/v	indoor	0.6/19.4
			5; 30	0.2 % w/v	outdoor	2/18
CS	2 methanol	S	5	0.06 % w/v	indoor	0.6/19.4
			5	0.2 % w/v	outdoor	2/18
CI	0.4000 ethanol	W	5	0.06 % w/v	indoor	0.6/19.4
			5; 30	0.2 % w/v	outdoor	2/18
A	0.4000 water	S	5	0.006 % w/v	indoor	0.3/19.7
			5; 30	0.02 % w/v	outdoor	1/19
A	5 methanol	W	5	0.4 % v/v	indoor	1.6/18.4
			5	1.5 % v/v	outdoor	6/14
A	5 methanol	S	5	0.4 % v/v	indoor	1.6/18.4
			5; 30	1.5 % v/v	outdoor	6/14
A	as supplied	W	5	5 % v/v	indoor	1/19
			5	5 % v/v	outdoor	1/19
A	as supplied	W	5	5 % v/v	indoor	1/19
			5; 30	5 % v/v	outdoor	1/19

The ABAs formulates (concentration in solution and in mixtures, type of solvent and coating) used for treatments are reported in Table 1, along with the curing time and samples expositions. The mixtures were freshly applied by brush on 5cm x 5cm and 1cm x 1cm marble specimens surface. The treatment consisted in four applications performed at intervals of 5 minutes, which correspond approximately to 200 g/m² of applied product. After application, both coatings (S and W) were let to cure 5 days at room temperature, in order to allow the release of ABAs active compounds and then the stone specimens were exposed to indoor (5cm x 5cm specimens) and outdoor conditions (1cm x 1cm specimens). Another set of marble samples (5cm x 5cm) treated with W coating containing ABAs were let to cure 30 days and exposed only under outdoor conditions.

Antifouling agents and coating characterization

A FT-IR spectrophotometer (Perkin Elmer System 2000) was used for the chemical characterization of the compounds. The solid products were detected using a diamond anvil cell, while the liquid ones were placed between KBr plates.

An ESEM (Quanta-200 FEI) environmental scanning electronic microscope equipped with EDX microanalysis system was used for elemental and morphological investigations. The microanalysis was performed acquiring data at 25 KeV, both at the pressure of 1 and 0.1 Torr; the quantitative data were calculated on the basis of a calibration curve. The ESEM-EDX system was used for observing the morphology and distribution of silicon based polymer (W), mixed or not with some natural antifouling agents (pAPS 0.005% w/v, A 5% v/v final concentration in coating), on Sivec marble specimens (5x5x1 cm³) after a curing time of 5 days (W-pAPS) and 30 days (W-A) at room temperature.

Growing conditions

The stone samples treated with low concentrations of ABAs were kept under laboratory controlled conditions, while the stone specimens treated with higher concentrations were exposed outdoor; in both cases the treated specimens were completely immersed in water containing mixed fouling phototrophic agents. The main growing conditions for both experiments are reported in the Table 2.

Table 2. Experimental conditions for efficiency evaluation of ABAs

Conditions	Indoor experiment	Outdoor experiment
Artificial basin	plastic container (33x27x13 cm) filled with freshwater	plastic container (150 cm diameter, 50 cm height) filled with freshwater
Substratum Exposure	Sivec marble (5x5x1 cm) low artificial lighting with continuous white fluorescent light at photosynthetic photon flux density of 10 $\mu\text{mol photon m}^{-2}\cdot\text{s}^{-1}$ in conditioned room at 27 °C	Sivec marble (1x1x0.5 cm and 5x5x1 cm) east orientation, day/night alternation, temperatures between 9°C and 37°C (average for T_{\min} and T_{\max} during the two months (June, July) of experiment being 17.4°C and 29.9 °C, respectively)
Inoculum	$\approx 2 \times 10^6$ cells/ml Enrichment of mixed natural biofilms composed by samples collected from two monumental fountains (The Second Fountain – Villa la Pietra, Florence, Italy and Sultana Fountain – Generalife, Granada, Spain). The main microorganisms were: green algae (<i>Cosmarium</i> sp., <i>Palmella</i> sp., <i>Chlorella</i> sp.), cyanobacteria (<i>Leptolyngbya</i> sp., <i>Aphanocapsa</i> sp., <i>Gloeocapsa</i> sp.), diatoms (<i>Nitzschia</i> sp.) and protozoa.	$\approx 1.6 \times 10^6$ cells/ml

Control of phototrophic growth

The autofluorescent signal of the phototrophs was detected by Epifluorescence microscopy (Nikon Eclipse E600, 4x and 10x objectives, TRITC filter with excitation 450-490 nm and emission in red region > 610 nm). The fluorescent images were photographed with a digital CCD camera (Nikon DXM1200F) and elaborated using a free image processing and analysis program (ImageJ[®]), available on-line [21] obtaining a two-dimensional semi-quantitative evaluation of phototrophic community's colonization on the stone specimens. 30 images, using 4x objective, were captured for the samples having 5cm x 5cm surface, while only 5 images, using 10x objective, for the samples with 1cm x 1cm surface. All the images were collected in RGB scale, consisting of 3840x3072 pixels (Fig. 1).

The raw images were opened and imported as JPG format (8-bit) and transformed to binary images (black/white) using the threshold adjust commands [20]. The optimum segmentation values were established for each photo by overlaying the original RGB image with the binary one, using Adobe Photoshop CS[®], in order to obtain an optimum black and

white image without losing information (Fig. 2). Later, the black spots, which are corresponding to fluorescent microorganisms, were analyzed with the same ImageJ[®] software, by measuring the covered area in each photo, and therefore a semi-quantification of the biological growth for each sample has been performed.

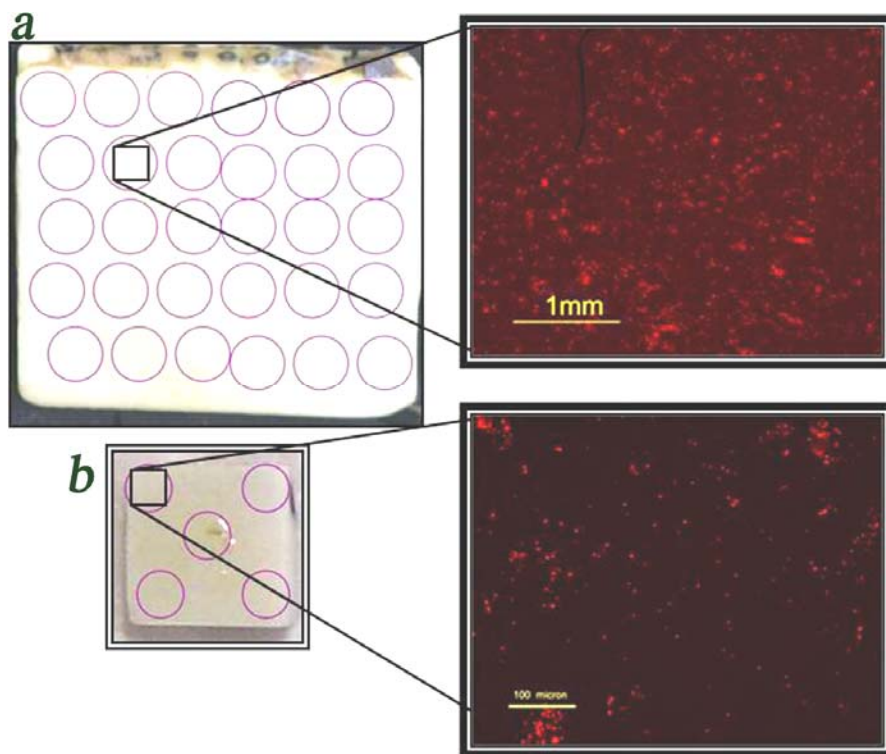


Fig. 1. Epifluorescence images capturing procedure for phototrophic biofilm analysis with 4x objective for 5x5 cm² samples (a) and 10x objectives for 1x1 cm² (b). The circle symbols represent the investigated areas on stone specimens.

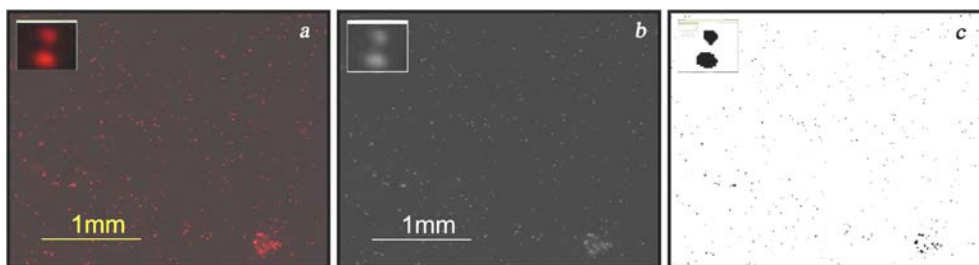


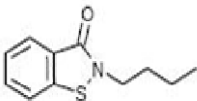
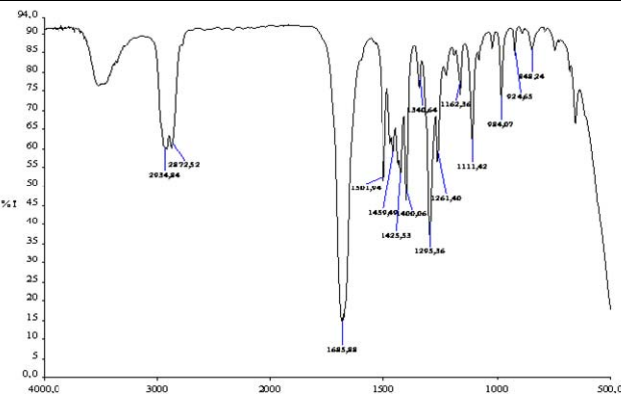
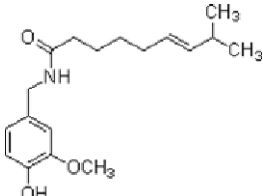
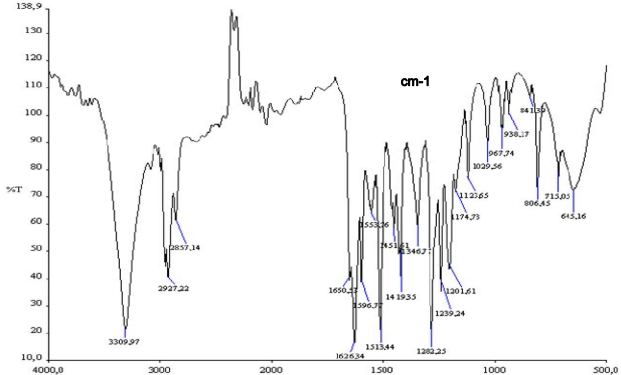
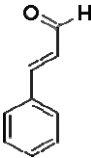
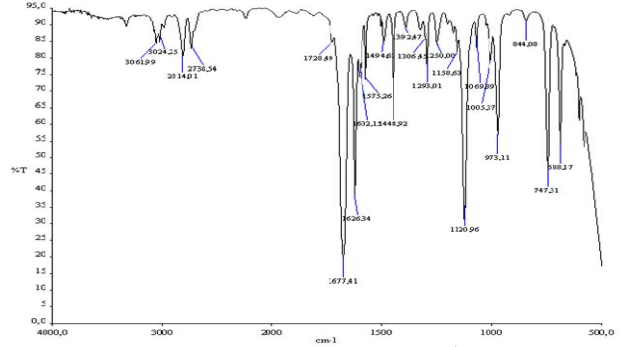
Fig. 2. Steps followed in epifluorescence image analysis: the normalized RGB image (a) was firstly converted in 8-bit gray scale (b) and then in a black and white binary image (c) which was segmented and analysed. The details show the quality of information to be analysed (red spot) which was not lost during conversion (black spot).

Results and discussion

ABAs and coatings characterization

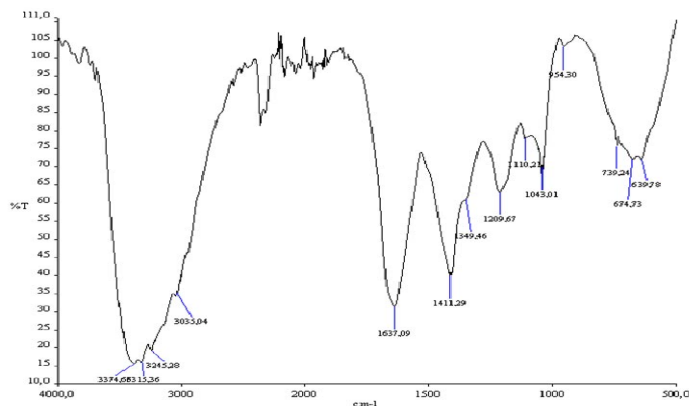
The original FT-IR spectra with the characteristic absorption peaks of the natural and commercial products are presented in Table 3.

Table 3. Structural formula and FTIR spectral characterization of the ABAs and coatings

ABAs/Coatings	FT-IR spectra
<p>AlgoPhase (A) <i>N-butyl-1,2-benzisothiazolin-3-one</i></p> 	 <p>Characteristic peaks: aliphatic C-H stretch. (2872 cm^{-1}, 2934 cm^{-1}), aliphatic C-H bending (1450 cm^{-1}, 1400 cm^{-1}, 1340 cm^{-1}), C=O stretch. (1685 cm^{-1}), aromatic C-C stretch (1501 cm^{-1}), aromatic out-of-plane C-H bending (984 cm^{-1}), C-N stretch. (1295 cm^{-1}) [26]</p>
<p>Capsaicin (CS) <i>8-methyl-N-vanillyl-6-nonenamide</i></p> 	 <p>Characteristic peaks: N-H stretch. (3310 cm^{-1}), aliphatic C-H stretch. (2927 cm^{-1}, 2857 cm^{-1}), C=O stretch. (1626 cm^{-1}), aromatic C-C stretch. (1596 cm^{-1}) and out-of-plane C-H bending (806 cm^{-1}), olefinic C=C stretch. (1650 cm^{-1}) and out-of-plane C-H bending (967 cm^{-1}), N-H bending and C-N stretch. (Amide II) (1513 cm^{-1}), asym C-O-C stretch (1282 cm^{-1}), C-O stretch (1202 cm^{-1}).</p>
<p>Cinnamaldehyde (CI) <i>Trans-3-phenyl-2-propenal</i></p> 	 <p>Characteristic peaks: Olefinic and aromatic C-H stretch. (3062 and 3024 cm^{-1}), olefinic C=C stretch (1626 cm^{-1}) and out-of-plane C-H bending (973 cm^{-1}), aromatic C-C stretch. (1602 and 1575 cm^{-1}) and out-of-plane C-H bending (747 and 688 cm^{-1}), aldehydic C-H stretch. (2814 and 2738 cm^{-1}), C=O stretch. (1677 cm^{-1}).</p>

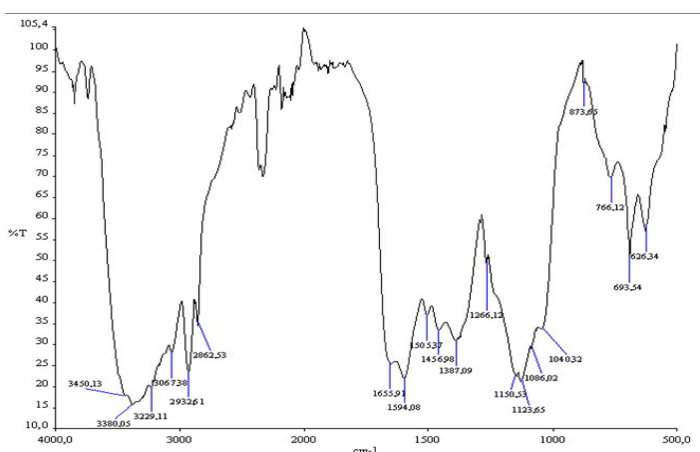
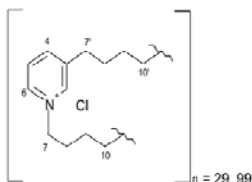
**Ceramium botryocarpum
extract (CBE)**

*Unknown active compound
(Hypothesis: salt of amino acids)*



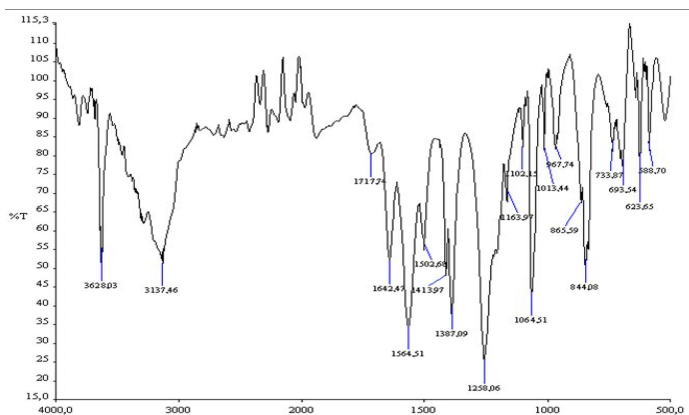
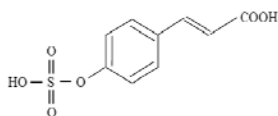
Characteristic peaks: N-H stretch. (range 3400-3200 cm^{-1}), asym COO^- stretch. and N-H bending (1637 cm^{-1}), sym COO^- stretch. (1411 cm^{-1}).

**Poly-alkylpyridinium salts
(pAPS)**



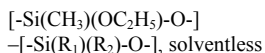
Characteristic peaks: Aliphatic C-H stretch. (2932 and 2862 cm^{-1}), aromatic C-H stretch. (3067 cm^{-1}), aromatic C-C (1594 cm^{-1}) and out-of-plane C-H bending (766 and 693 cm^{-1}). The strong signals in the range 3500 - 3000 cm^{-1} and at 1656 cm^{-1} may be due to water. The product is not pure.

**Zosteric acid (ZA)
p-sulphoxy-cinnamic acid**

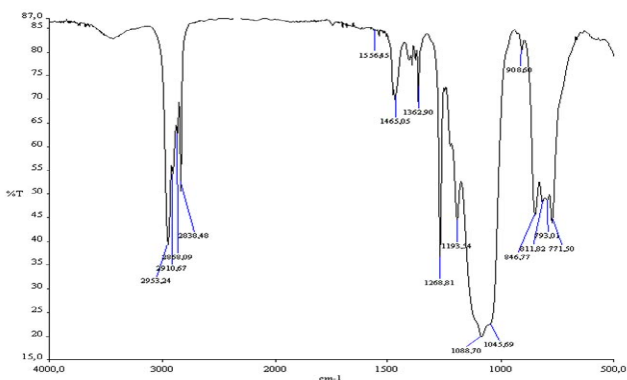


Characteristic peaks: O-H stretch. of sulphonyl group (3628 cm^{-1}), O-H stretch of carboxylic group (3137 cm^{-1}), C=O stretch. (1717 cm^{-1}), olefinic C=C (1642 cm^{-1}) and out-of-plane C-H bending (967 cm^{-1}), asym COO^- stretch. (1564 cm^{-1}) and sym COO^- stretch. (1387 cm^{-1}), S=O stretch. (1064 cm^{-1}), *p*-substituted aromatic out-of-plane C-H bending (844 cm^{-1}). The compound is not pure.

Silres BS 290
(pure W)

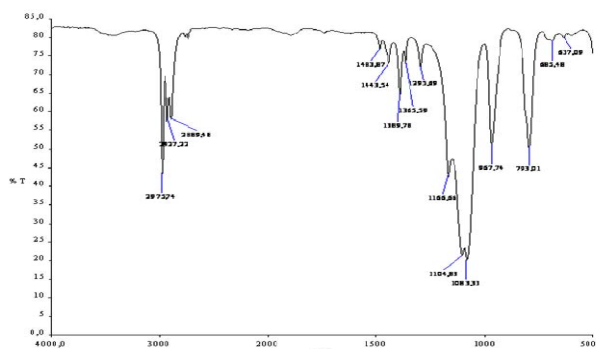


$\text{R}_1, \text{R}_2 = \text{alkyl groups}$



Characteristic peaks: Aliphatic C-H stretch. (2953 and 2838 cm^{-1}), CH_3 bending in $\text{Si}(\text{CH}_3)_x$ (1269 cm^{-1}), Si-O stretch. (range 1100-1000 cm^{-1}), in-plane $(-\text{CH}_3)$ bending in Si-O-R (1193 cm^{-1}), Si-C stretch. (847 cm^{-1}) and in-plane (CH_3) bending in $-\text{O-Si}(\text{CH}_3)\text{-O}$ (771 cm^{-1}) [27].

Silres BS OH 100 (S)



Characteristic peaks: aliphatic C-H stretch. (2976, 2927 and 2889 cm^{-1}), asym Si-O-C stretch. (range 1110-1000 cm^{-1}), sym Si-O-C stretch. (968 cm^{-1}), in-plane CH_2 bending (793 cm^{-1}).

The presence of ABAs mixed with silicones it is hardly evidenced by FT-IR analysis. This is due to the very low concentration used and/or because the characteristic regions for ABAs spectra are overlaid by that ones of W which has strong signals between 1300-800 cm^{-1} . However for CI and A, the characteristic signals of the ABAs agent were detected in the mixture, and it seems that CI reacts with the W coating, while A seems undergo some chemical modifications without reacting with the coating (Fig. 3, Fig. 4). In fact, the signals involving the Si-O bond (in the region 1100-1000 cm^{-1}) and the in-plane $-\text{CH}_3$ bending in the $-\text{O-Si}(\text{CH}_3)\text{-O}$ bond (around 775 cm^{-1}) show different wavenumber and relative intensity when the spectrum is obtained from W coating or from W + CI (Fig. 3a). On the other hand, the FT-IR signals due to the Si- CH_3 bonds (around 1270 and 847 cm^{-1}) remained unchanged in W and W + CI coatings. This is in accordance with a structure where the Si- CH_3 group do not feel the effects of the reacted aldehydic group since its distance from the reactive center. The presence of the signal at 1677 cm^{-1} in the W + CI coating (C=O stretch of CI) states the incomplete reaction of CI with W.

On the contrary, in the case of Algophase (A) incorporated in W, the signals due to the silicon based polymer are comparable to those obtained with the pure W coating (Fig. 4). The modifications observed in the FT-IR spectrum may be explained with a transformation of A but not with a reaction between the coating and Algophase.

In Fig. 5 the ESEM microphotographs of the W coating, mixed or not with A and pAPS, at two different curing times are shown. W coating, cured for 30 days, forms on the stone surface a continuous film, while that one cured only for 5 days has a broke up aspect, with small

holes, probably due to its partial gelification and to the residual solvent removal during the ESEM analysis. Similar morphological aspect was also observed for the mixtures W-A and W-pAPS cured for 5 days as well. On the contrary the morphology of the W coating containing the pAPS shows the presence of non-continuous film also after 30 days of curing. This may be due to the water, used as a solvent for pAPS dissolution; the mixture used for this treatment, in fact, contained about 30% H₂O and 70% W.

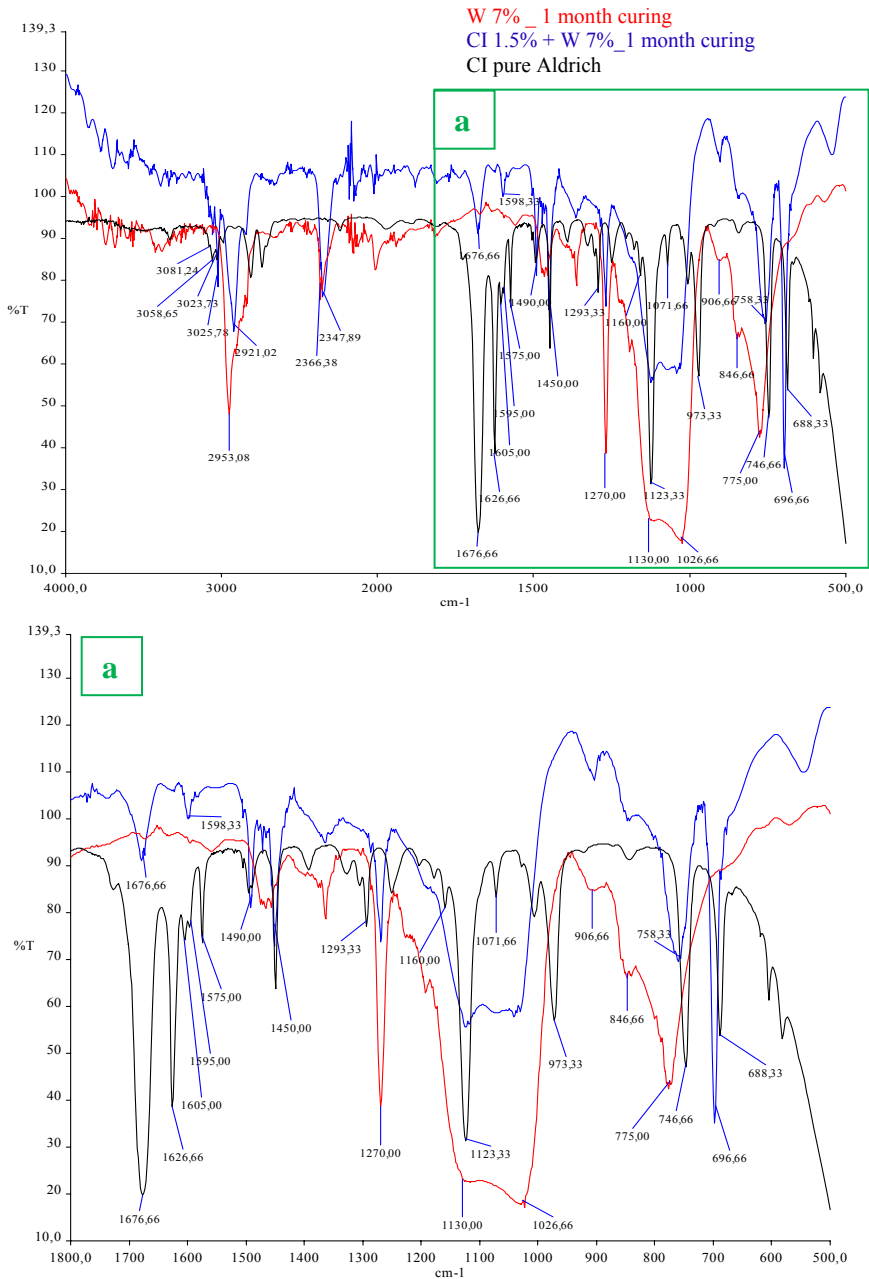


Fig. 3. The FT-IR spectra of Cinnamaldehyde incorporated into Silres BS 290 coating after 1 month of curing with detail of the 1800-500 cm⁻¹ region.(a)

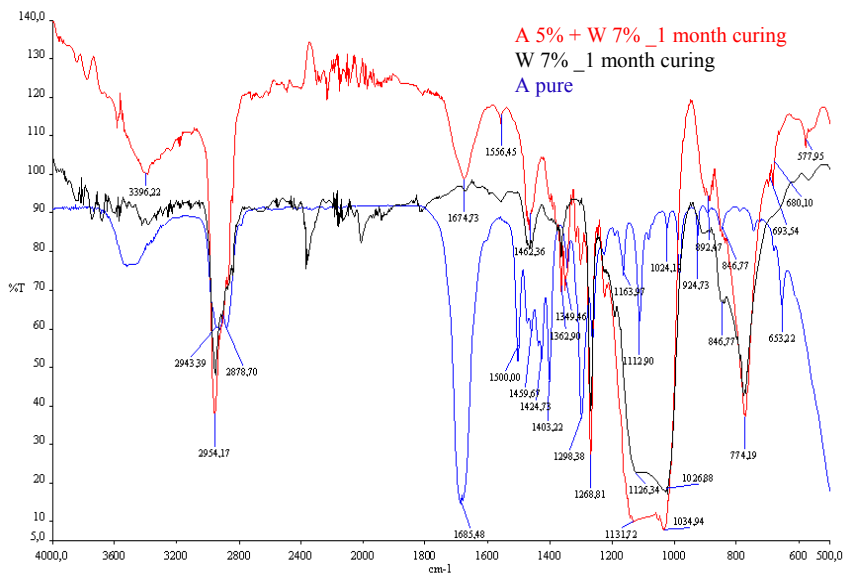


Fig. 4. The FT-IR spectra of AlgoPhase incorporated into Silres BS 290 coating after 1 month of curing,.

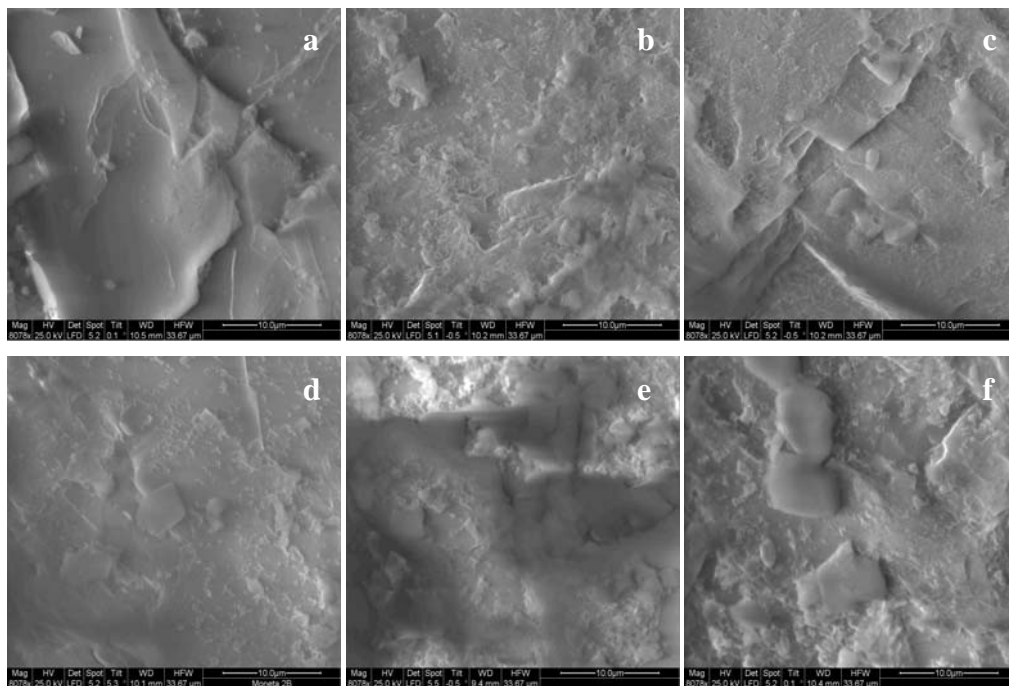


Fig 5. ESEM micrographs with the surface morphology of the treatments applied on Sivec marble specimens: (a) stone surface without any treatment; (b) with W cured for 5 days; (c), with W cured for 30 days; (d), with W+A cured for 5 days; (e), with W+pAPS cured for 5 days; (f), with W+pAPS cured for 30 days.

The ESEM-EDX analysis showed, for all the treatments, an increase of silicon content on the stone surface (Table 4). The less amount of silicon found on the specimens coated with W-pAPS and W-A is in accordance with the lower concentration of W in the treatment solutions.

Table 4. ESEM-EDX analysis performed on the surface of Sivec marble treated with different coatings after two curing periods (5 and 30 days). Untreated Sivec marble is also reported for comparison.

Element (%Atom)	Sivec Marble	W (5 days curing)	W (30 days curing)	W+pAPS (5 days curing)	W+pAPS (30 days curing)	W+A (5 days curing)
C	30.3 (±0.7)	33.8 (±3.8)	30.9 (±2.0)	28.8 (±5.3)	28.6 (±2.3)	31.1 (±2.3)
O	50.2 (±0.1)	48.7 (±3.2)	50.1 (±1.1)	49.4 (±1.4)	48.6 (±2.3)	50.3 (±0.5)
Mg	107 (±0.1)	7.9 (±1.1)	8.9 (±0.8)	8.3 (±3.2)	7.3 (±3.0)	9.4 (±0.7)
Si	0.1 (±0.0)	1.3 (±0.9)	1.6 (±0.5)	0.7 (±0.4)	0.7 (±0.2)	0.9 (±0.7)
Ca	8.8 (±0.6)	8.2 (±0.9)	8.5 (±1.3)	12.8 (±7.2)	14.8 (±3.9)	8.4 (±2.1)
Total	100	100	100	100	100	100

ABAs' efficacy

Indoor Experiment

The inhibition efficiency of all the ABAs incorporated both in W and S, observed during the first month, is very low (Fig. 6), even if the W coating seems to assist the efficiency of ABAs. In the second month, the phototrophic growth, with diatoms dominant, was higher than the reference in all the treated specimens. This result may be explained with the low concentration of ABAs in the coatings, as well as with the presence of silicon that can be used for the growth of diatoms frustule. As observed for the first month, the reactivity of the S coatings with the fouled water is higher than the W ones; in addition it must be pointed out that the standard deviation of the measures (% of covered area) in the case of the S coatings is always higher than in the case of W coatings. This means that the surface is more discontinuous, probably due to the detachments of biofilm together or not with small parts of the coating.

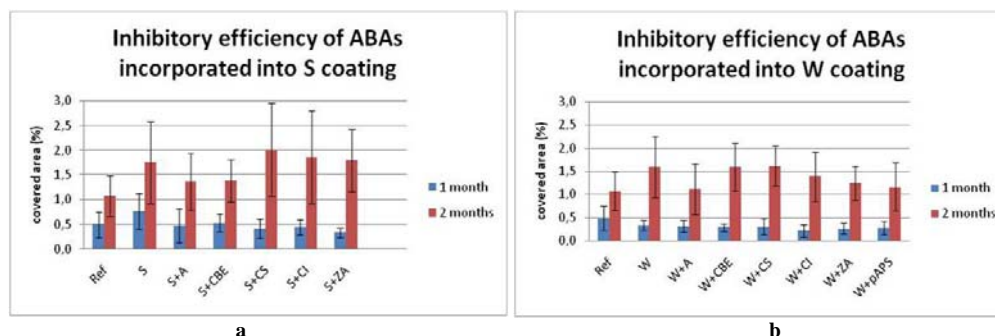


Fig 6. Inhibitory efficiency of ABAs incorporated into Silres BS OH 100 (S) (a) and Silres BS 290 (W) (b) coatings applied on Sivec marble specimens under indoor conditions. Curing time = 5 days.

Outdoor Experiments

Some of the ABAs (CI, CS and pAPS) incorporated into both types of coatings (W, S) seem to have a good inhibitory impact on the biofilm growth in the first 15 days of its

development (Fig. 7). After the first and the second month, some treated stone specimens with S coating containing or not ABAs (S-A, S-CBE, S) showed a surprising diminution of the patina; the same effect was not observed in the reference and in the correspondent W-ABAs coatings (Fig. 7b). This not expected behaviour may be ascribed to the swelling, in water, of the silica formed by gelification of the S based coatings, as well as to a poor compatibility (poor adhesive effect) between the stone (calcium magnesium carbonate, dolomite) and silica gel, which cause the random detachment of the microbiological patina and/or the silica gel. The W carrier with pAPS, CI and CS demonstrated a good inhibitory effect on phototrophic growing even after 2 months of immersion. W without ABAs seems to have a little inhibitory effect in the first 15 days, but after 2 months the growth of the phototrophic biofilm on this coating was similar to that observed on the untreated specimens (Fig. 7).

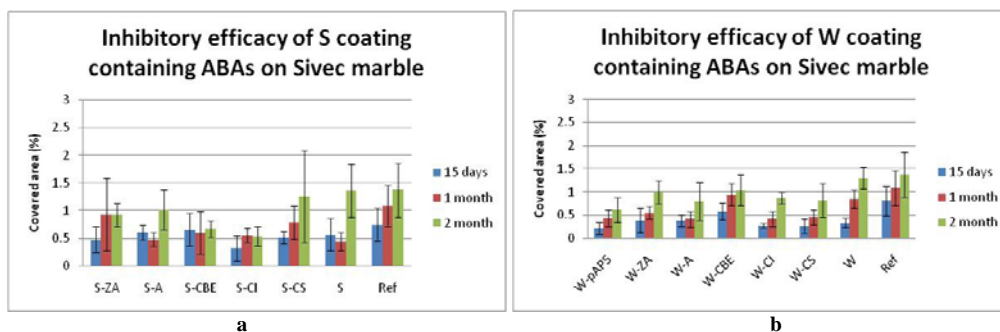


Fig 7. Efficiency of ABAs incorporated into Silres BS OH 100 (a) and Silres BS 290 (b) coating applied on Sivec marble specimens under outdoor conditions. Curing time = 5 days.

As regard the treatments cured for 1 months and tested under outdoor exposition, the results revealed a wide phototrophic growth, both on the reference (untreated specimen) and on all coated stone specimens (containing or not ABAs). The wide growth was observed even after 15 days of water immersion. After 30 days of immersion, the biological development could be seen by naked eye. These results led to the assumption that the complete curing of the incorporating agent Silres BS 290 blocks the ABAs action.

Conclusions

The results obtained on these preliminary experiments are quite encouraging for the use of some antibioulfing agents (CI and pAPS) as potential effective products against biofilm formation. The W coating (Silres BS 290) showed better performances than S coating (Silres BS OH 100) as incorporating agent, but only when incompletely cured. The short curing period (5 days) does not prevent the action of the ABAs inhibitors, however this partial curing most probably favors the coating removal by water with the consequent elimination of the ABAs active products.

The complete curing of W coating containing ABAs (30 days) did not show any preventive action against biofilm formation. This can be due to: (i) the loosening/lacking of leaching properties for W to release ABAs and/or (ii) the occurrence of a chemical reaction between the ABAs and coating, with subsequent changes of their inhibitory properties and hence, more suitable supporting product must be investigated.

Therefore, further detailed studies for defining the optimal concentration and the best condition for a constant releasing and long lasting of incorporated ABAs are a key point for similar researches.

Acknowledgments

The authors thank to K. Sepčić (Univ. of Ljubljana, Biotechnical Faculty, Slovenia) and A. Bazes (Univ. of South-Bretagne, LBCM, France) for natural extracts supplying and to G. Schonaut (ACR Restauro, Venice, Italy) for research theme suggestion. This work has been made in the frame of the EPISCON Project (MEST-CT-2005-020559 - European PhD in Science for Conservation).

References

- [1] Th. Warscheid, J. Braams, *Biodeterioration of stone: a review*, **International Biodeterioration and Biodegradation**, **46**, 4, 2000, pp.343-368.
- [2] L. Tomaselli, G. Lamenti, M. Bosco, P. Tiano, *Biodiversity of photosynthetic micro-organisms dwelling on stone monuments*, **International Biodeterioration and Biodegradation**, **46**, 3, 2000, pp. 251-258.
- [3] L.V. Evans, N. Clarkson, *Antifouling strategies in the marine environment*, **Journal of Applied Bacteriology, Symposium Supplement**, **74**, 1993, pp. 119S-124S.
- [4] N. Fusetani, *Biofouling and antifouling*, **Natural Product Reports**, **21**, 2004, pp. 94-104.
- [5] L.D. Chambers, K. R. Stokes, F.C. Walsh, R.J.K. Wood, *Modern approaches to marine antifouling coatings*, **Surface & Coatings Technology**, **201**, 2006, pp. 3642-3652.
- [6] R. de Nys, P.D. Steinberg, *Linking marine biology and biotechnology*, **Current Opinion in Biotechnology**, **13**, 2002, pp. 244-248.
- [7] D.M. Yebra, S. Kiil, K. Dam-Johansen, *Antifouling technology – past, present and future steps towards efficient and environmentally friendly antifouling coatings*, **Progress in Organic Coatings**, **50**, 2004, pp. 75-104.
- [8] T. Geiger, P. Delavy, R. Hany, J. Schleuniger, M. Zinn, *Encapsulated zosteric acid embedded in poly[3-hydroxyalkanoate] coatings – protection against biofouling*, **Polymer Bulletin**, **52**, 2004, pp. 65-72.
- [9] R. Hany, C. Bohlen, T. Geiger, M. Schmid, M. Zinn, *Toward non-toxic antifouling; synthesis of hydroxy-, cinnamic acid-, sulphate-, and zosteric acid-labeled poly[3-hydroxyalkanoates]*, **Biomacromolecules**, **5**, 2004, pp. 1452-1456.
- [10] C. A. Barrios, *Incorporation of zosteric acid into silicone coatings to deter fresh water bacteria attachment*, Master of Science Thesis, University of Akron, Ohio, Canada, 2004, p. 1-139.
- [11] Q. Xu, C.A. Barrios, T. Cutright, B.Z. Newby, *Assessment of antifouling effectiveness of two natural product antifoulants by attachment study with freshwater bacteria*, **Environmental Science and Pollution Research International**, **12**, 5, 2005, pp. 278-284.
- [12] B.Z. Newby, T. Cutright, C.A. Barrios, Q. Xu, *Zosteric acid – an effective antifoulant for reducing fresh water bacterial attachment on coatings*, **Journal of Coatings Technology Research**, **3**, 1, 2006, pp. 69-76.
- [13] K. Sepčić, G. Guella, I. Mancini, F. Pietra, M. Dalla Serra, G. Manestrina, K. Tubbs, P. Maček, T. Turk, *Characterization of anticholinesterase-active 3-alkylpyridinium polymers from the marine sponge Reniera sarai in aqueous solutions*, **Journal of Natural Products**, **60**, 1997, pp. 991-996.
- [14] K. Sepčić, T. Turk, *3-Alkylpyridinium compounds as potential non-toxic antifouling agents*, **Progress in Molecular and Subcellular Biology**, **42**, 2006, pp. 105-124.

- [15] J.S. Todd, R.C. Zimmerman, Ph. Crews, R.S. Alberte, *The antifouling activity of natural and synthetic phenol acid sulphate esters*, **Phytochemistry**, **34**, 1993, pp. 401-404.
- [16] A. Bazes, A. Silkina, D. Defer, C. Bernède-Bauduin, E. Quémener, J.P. Braud, N. Bourgougnon, *Active substances from *Ceramium botryocarpum* used as antifouling products in aquaculture*, **Aquaculture**, **258**, 2006, pp. 664-674.
- [17] J.L. Watt, Patent US5397385 (A)/1995.
- [18] H.C. Lee, S.S. Cheng, S.T. Chang, *Antifungal property of the essential oils and their constituents from *Cinnamomum osmophloeum* leaf against tree pathogenic fungi*, **Journal of the Science of Food and Agriculture**, **85**, 2005, pp. 2047-2053.
- [19] C. Niu, A. Gilbert, E.S. Gilbert, *Subinhibitory concentrations of cinnamaldehyde interfere with quorum sensing*, **Letters in Applied Microbiology**, **43**, 2006, pp. 489-494.
- [20] M.E. Sieracki, C.L. Viles, *Color image-analyzed fluorescence microscopy: a new tool for marine microbial ecology*, **Oceanography**, **3**, 990, pp. 30-36.
- [21] <http://www.rsbweb.nih.gov/ij/>
- [22] S.D. Alexandratos, **Patent US5990336 (A)/1999**.
- [23] A. Claude, S. Bondu, F. Michaud, N. Bourgougnon, E. Deslandes, *X-ray structure of a sodium salt of digeneaside isolated from red alga *Ceramium botryocarpum**, **Carbohydrate Research**, **344**, 5, 2009, pp. 707-710.
- [24] C. Turgut, B.M. Newby, T.J. Cutright, *Determination of optimal water solubility of capsaicin for its usage as non-toxic antifoulant*, **Environmental Science and Pollution Research International**, **11**, 1, 2004, pp. 7-10.
- [25] L.L. Chia, E.F. Warwick, **Patent US0197366 (A)/2005**.
- [26] R.M. Silverstein, F.X. Webster, **Spectrometric identification of organic compounds** (sixth edition), John Wiley & Sons, Inc., New York, 1998, p. 82-108.
- [27] C.D. Craver, **The Coblentz Society Desk Book of Infrared Spectra** (second edition), The Coblentz Society, Kirkwood, Missouri, 1977, p. 1-498.
-

Received: December 25, 2010

Accepted: January 27, 2011